



# Inter-fraction dynamics during post-operative 5 fraction cavity hypofractionated stereotactic radiotherapy with a MR LINAC: a prospective serial imaging study

Hendrick Tan<sup>1,4</sup> · James Stewart<sup>1</sup> · Mark Ruschin<sup>2,3</sup> · Michael H. Wang<sup>1</sup> · Sten Myrehaug<sup>1,2</sup> · Chia-Lin Tseng<sup>1,2</sup> · Jay Detsky<sup>1,2</sup> · Zain Husain<sup>1,2</sup> · Hanbo Chen<sup>1,2</sup> · Arjun Sahgal<sup>1,2</sup> · Hany Soliman<sup>1,2</sup> 

Received: 30 October 2021 / Accepted: 27 December 2021 / Published online: 3 January 2022  
© The Author(s), under exclusive licence to Springer Science+Business Media, LLC, part of Springer Nature 2022

## Abstract

**Purpose/Objective(s)** This study examined changes in the clinical target volume (CTV) and associated clinical implications on a magnetic resonance imaging linear accelerator (MR LINAC) during hypofractionated stereotactic radiotherapy (HSRT) to resected brain metastases. In addition, the suitability of using T2/FLAIR (T2f) sequence to define CTV was explored by assessing contouring variability between gadolinium-enhanced T1 (T1c) and T2f sequences.

**Materials/Methods** Fifteen patients treated to either 27.5 or 30 Gy with five fraction HSRT were imaged with T1c and T2f sequences during treatment; T1c was acquired at planning (FxSim), and fraction 3 (Fx3), and T2f was acquired at FxSim and all five fractions. The CTV were contoured on all acquired images. Inter-fraction cavity dynamics and CTV contouring variability were quantified using absolute volume, Dice similarity coefficient (DSC), and Hausdorff distance (HD) metrics.

**Results** The median CTV on T1c and T2f sequences at FxSim were 12.0cm<sup>3</sup> (range, 1.2–30.1) and 10.2cm<sup>3</sup> (range, 2.9–27.9), respectively. At Fx3, the median CTV decreased in both sequences to 9.3cm<sup>3</sup> (range, 3.7–25.9) and 8.6cm<sup>3</sup> (range, 3.3–22.5), translating to a median % relative reduction of –11.4% on T1c (p=0.009) and –8.4% on T2f (p=0.032). We observed a median % relative reduction in CTV between T1c and T2f at FxSim of –6.0% (p=0.040). The mean DSC was 0.85 ± 0.10, and the mean HD was 5.3 ± 2.7 mm when comparing CTV on T1c and T2f at FxSim.

**Conclusion** Statistically significant reductions in cavity CTV was observed during HSRT, supporting the use of MR image guided radiation therapy and treatment adaptation to mitigate toxicity. Significant CTV contouring variability was seen between T1c and T2f sequences.

*Trial registration* NCT04075305 – August 30, 2019

**Keywords** Brain metastases · Hypofractionated stereotactic radiotherapy · Magnetic resonance image-guided radiotherapy · Adaptive radiotherapy

The results of the study were presented at the 16th MR Linac Consortium meeting in June 2021 and the 63rd annual meeting of the American Society for Radiation Oncology (ASTRO) in Oct 2021.

✉ Hany Soliman  
hany.soliman@sunnybrook.ca

<sup>1</sup> Department of Radiation Oncology, Odette Cancer Centre, Sunnybrook Health Sciences Centre, 2075 Bayview Avenue, Toronto, ON M4N 3M5, Canada

<sup>2</sup> Department of Radiation Oncology, University of Toronto, Toronto, Canada

<sup>3</sup> Department of Medical Physics, Sunnybrook Odette Cancer Centre, Toronto, Canada

<sup>4</sup> GenesisCare, Perth, WA, Australia

## Introduction

Surgical resection is essential in the treatment paradigm of large or symptomatic brain metastases and has been demonstrated to improve survival for patients with solitary metastasis [1]. Postoperative whole brain radiation therapy (WBRT) has historically been the standard of care to minimize local recurrence, but it is associated with a clinically significant decrease in neurocognitive function [2–4]. Hence, there has been a shift towards the use of stereotactic radiosurgery (SRS) [5, 6] and hypofractionated stereotactic radiotherapy (HSRT) [7, 8] to the resected cavity to mitigate neurocognitive toxicity.

In the above context, consensus contouring guidelines have established CTV definitions based on gadolinium-enhanced T1 (T1c) magnetic resonance imaging (MRI) sequence [9]. Given that the target is typically a thin rim of “normal” brain tissue, accurate target delineation is essential to optimize the therapeutic ratio, reduce the risk of radionecrosis (RN), and allow for dose escalation [7, 10–12]. A recent publication by Teyateeti et al. has concluded that T2 weighted MRI could provide an accurate resection cavity delineation without any detrimental clinical implications [13]. In order to determine the ideal sequence for cavity delineation, we assess the suitability of using T2/FLAIR (T2f) sequences as a surrogate to define CTV was explored by assessing contouring variability between these two sequences acquired at the same time point.

However, even with consistent contouring practices, inter-fraction cavity dynamics can limit the therapeutic efficacy of high-precision radiotherapy techniques and potentially increase the risk of symptomatic RN. To date, monitoring of resected cavities during treatment is not the standard of practice, but since the inception of MRI linear accelerators (MR LINAC), daily target visualization can now be integrated into treatment [14]. In the present study, we also quantify the inter-fraction cavity dynamic changes and the potential correlation between CTV volume change and clinical implications on a 1.5 T MRI linear accelerator (Elekta Unity, Elekta AB, Stockholm, Sweden).

## Methods

### Patient characteristics and treatment workflow

Fifteen postoperative resected brain metastases patients were included in this ethics board-approved trial, the MOMENTUM study (Clinicaltrials.gov: NCT04075305) which is a prospective registry trial with specific central nervous system module and defined follow-up parameters [15]. All patients had undergone a gross total resection (GTR) before planned HSRT with a 5-fraction regimen. The indication for surgical resection was based upon tumor size, location, patient performance status, life expectancy, and symptoms associated with brain metastases. Patient characteristics are summarized in Table 1.

All CTV contours were concordant with the international postoperative cavity consensus contouring guideline [9]. A 2 mm volumetric margin expansion beyond CTV was used to define the planning target volume (PTV). All patients were treated with either 27.5 Gy or 30 Gy in 5 daily fractions delivered to the PTV. Treatment planning consisted of generating an initial reference plan, with the dosimetric criteria of > 98% of PTV receiving the prescribed dose (i.e. V100 > 98%). On each of the 5 daily

**Table 1** Patient and tumor characteristics

Characteristic	Number
Number of patients	15
Median age in years (range)	59 (44–66)
Median time from surgery to HSRT in days (range)	22 (15–31)
Gender	
Female	9 (60%)
Male	6 (40%)
Tumor histology	
Breast	6 (40%)
Non-small cell lung cancer (NSCLC)	5 (33.3%)
Colorectal adenocarcinoma	2 (13.3%)
Renal cell	1 (6.7%)
Uterine sarcoma	1 (6.7%)
Extent of resection	
Gross total	15
ECOG	
1	13 (86.7%)
2	2 (13.3%)
Cavity dimension	
< 10 cc	7 (46.7%)
10–20 cc	5 (33.3%)
> 20 cc	3 (20%)
5 fraction total dose	
27.5 Gy	5 (33.3%)
30 Gy	10 (66.7%)
Previous brain radiation	
Yes	2 (13.3%)
No	13 (86.7%)
Tumor location	
Supratentorial	11 (73.3%)
Infratentorial	4 (26.7%)
Targeted agent or immunotherapy after HSRT	
Yes	2 (13.3%)
No	13 (86.7%)

fractions, the adapt-to-position (ATP) workflow on the MR LINAC was followed, in which a translation-only fusion between reference image and daily T1 was used to update the isocentre location, and the beams segments were re-optimized to re-capitulate the original reference plan as close as possible, without accounting for any changes to the CTV. Retrospectively, the CTV was re-contoured on Fx3 and the new contour was used to generate target coverage using the original, unaltered, reference plan and compared to those same metrics using the original FxSim contours. Dosimetric data, including the total volume of brain minus CTV receiving 30 Gy (V30Gy), and 25 Gy (V25Gy) were recorded from the reference plan. The adapt-to-shape (ATS) workflow, whereby plan adaptation

and optimization is based on the new changes to CTV and anatomy was not utilised, even if volumetric change was noted on Fx3.

Patients were simulated with a 1.5 T Phillips Ingenia system using T1c and T2f sequences. The imaging protocol consisted of T1c at the time of planning (FxSim) and at fraction 3 (Fx3), T2f at FxSim, and all five fractions during HSRT. Fx3 was chosen to perform a T1c sequence as this represents the midway mark of HSRT and was felt to be a convenient time point to capture changes in cavity dynamics. FxSim MRI was obtained at a median time of 15 days after surgery (range, 9–23 days). HSRT was commenced at a median of 7 days (range, 3–18 days) following FxSim MRI, and Fx3 MRI was obtained at a median time of 25 days after surgery (range, 16–33 days). With regards to MRI images, the MR LINAC system uses a modified MRI scanner based on the Philips Marlin MRI. Both the MR LINAC and MRI simulator scanners were fully commissioned in accordance with The American Association of Physicists in Medicine (AAPM) Report 100, and American College of Radiology (ACR) recommendations, which cover (with tolerances) geometric accuracy ( $\pm 2$  mm), high-contrast spatial resolution ( $\leq 1.0$  mm), slice thickness accuracy ( $5.0$  mm  $\pm 0.7$  mm), slice position accuracy ( $\leq 5$  mm), image intensity uniform ( $\geq 87.5\%$ ), percent-signal ghosting ( $\leq 2.5\%$ ), and low-contrast object detectability ( $\geq 9$  total spokes on ACR phantom) and gradient linearity (% geometric distortion  $< 2\%$ ). Our daily MRI QA tests include tests for signal-to-noise ratio (SNR) and scaling accuracy in accordance with national and international guidelines. In general, the MR LINAC scanner performs similarly to the MR simulator scanner, but with lower SNR due to the adjustments made to the gradient coils to accommodate the linear accelerator, as well as the lack of a head coil. The T1 sequence on the MR simulator has a  $0.5$  mm  $\times$   $0.5$  mm in plane resolution and  $1$  mm slice thickness whereas the MR LINAC T1 sequence has a  $0.7$  mm  $\times$   $0.7$  mm in plane resolution and  $1.1$  mm slice thickness. The MR LINAC T2f sequence has an in plane resolution of  $0.5$  mm  $\times$   $0.5$  mm and slice thickness of  $1.3$  mm.

### Target delineation

CTVs were contoured on T1c sequences at FxSim and Fx3 using the Monaco treatment planning system (Monaco v.5.40.0.1; Elekta AB, Stockholm, Sweden) as per the consensus guidelines [9]. CTVs were also defined on T2f sequences at FxSim and all five fractions during HSRT. Generally, the T2 signal hyperintensity surrounding the surgical cavity was not included into the CTV volume.

Two radiation oncologists independently reviewed all volumes to ensure consistency before analysis.

### Cavity dynamics assessment and CTV contouring variability

Cavity dynamics were quantified using CTVs on T1c sequences at FxSim and Fx3. The CTV was also contoured on T2f sequences at FxSim and all five fractions during HSRT to evaluate the change with each fraction and to compare the T1c contours at FxSim and Fx3. All contours were rigidly co-registered to their FxSim images. The metrics used to quantify T1c and T2f CTV dynamics and variability were as follows:

- (1) Absolute and relative volumes of the CTV on both the T1c and T2f images. Relative volumes were expressed as a percentage of the volume at FxSim, with positive and negative values indicating enlargement and reduction, respectively. Additionally, for each CTV, the spatial distribution of centroid, compared to the centroid of reference volume at FxSim, was analyzed. A mean CTV centroid of analyzed volumes on T1c for Fx3 and T2f for all five fractions was calculated to measure the distance relative to centroid reference volumes at FxSim.
- (2) Dice similarity coefficient (DSC) was used to measure the overlap between T1c and T2f CTV contours at FxSim and Fx3. The Dice similarity coefficient measures the degree of overlap of the two volumes and, for three-dimensional regions A and B, is calculated as:

$$DSC = 2 \times \frac{|A \cap B|}{|A| + |B|}$$

where  $|A \cap B|$  is the intersection of regions A and B and  $| \bullet |$  denotes the volume of the given region. The DSC has a value of 1 when two contours are entirely coincident and a value of 0 when the two contours are entirely disparate, with no region of overlap.

- (3) Hausdorff distance (HD) metrics were used to consider distance differences between T1c and T2f CTV contours. Given two regions A and B, HD is defined as:

$$HD(A, B) = \max(h(A, B), h(B, A))$$

where

$$h(A, B) = \max_{a \in A} \min_{b \in B} \|a - b\|$$

Essentially, the HD describes the most mismatched distance of a point from A to B. If  $HD(A, B) = d$ , for example, then every point within A must be within distance  $d$  of the nearest point within B and vice versa.

## Follow up and statistical analysis

Two months after HSRT, a volumetric T1c MRI was followed by a clinic visit. Thereafter, MRIs and follow-up visits were repeated every 2–3 months. At each follow-up, radiation effects, including RN (either symptomatic or asymptomatic) were recorded based on the criteria defined by Sneed et al. [16].

Continuous data were summarized using mean and standard deviation (SD) or median and range, and categorical data using frequency counts or percentages. Statistical analysis was performed using two-sided paired t-test. Univariable and multivariable testing was not performed due to the small sample size and low event rates. A p-value of 0.05 was defined as the threshold for statistical significance.

## Results

### Cavity dynamics assessment

#### Absolute and relative volume

We observed a reduction in CTV in 12/15 (80%) patients on T1c at Fx3 relative to FxSim. The median CTVs on T1c at FxSim and Fx3 were  $12.0\text{cm}^3$  (range, 1.2–30.1) and  $9.3\text{cm}^3$  (range, 3.7–25.9), respectively which translate to a median % relative change in CTV of  $-11.4\%$  (range,  $-24.9\%$  to  $+7.1\%$ ) between the two time points. Relative to FxSim, this reduction was statistically significant,  $p=0.009$ . Three patients (20%) had an increase in CTV

between FxSim and Fx3, reflecting a median % relative change in CTV of  $+7.0\%$  (range,  $+2.5\%$  to  $+7.1\%$ ). The median CTVs on T2f at FxSim and Fx3 were  $10.2\text{cm}^3$  (range, 2.9–27.9) and  $8.6\text{cm}^3$  (range, 3.3–22.5), respectively translating to a median % relative change in CTV of  $-8.4\%$  (range,  $-21.8$  to  $+55.6\%$ ) ( $p=0.032$ ). Figure 1a illustrates the CTV volume on T1c at FxSim and Fx3 and T2f at FxSim and all five fractions, (b) refers to the CTV volume change and (c) shows the CTV centroid displacement on T1c at Fx3 and T2f at all five fractions relative to FxSim.

### Volume change vs clinical implications

The mean V30Gy, and V25Gy for all patients at FxSim were  $6.1 \pm 4.6\text{cm}^3$  (mean  $\pm$  SD), and  $21.8 \pm 8.2\text{cm}^3$ , respectively. We observed an increase in the mean V30Gy, and V25Gy at Fx3,  $7.2 \pm 5.5\text{cm}^3$  and  $23.2 \pm 9.4\text{cm}^3$ , respectively. Relative to FxSim, this increase was statistically significant,  $p=0.008$ . Overall, 12/15 patients recorded a reduction in CTV on T1c at Fx3 relative to FxSim. Two of twelve patients with a reduction in CTV at Fx3 developed asymptomatic RN on follow up MRI, of which one patient had previously received hippocampal avoidance WBRT. The second patient with RN recorded the largest V30Gy and V25Gy amongst all patients, both at FxSim (V30Gy =  $15.7\text{cm}^3$ , V25Gy =  $37.5\text{cm}^3$ ) and Fx3 (V30Gy =  $20.1\text{cm}^3$ , V25Gy =  $41.8\text{cm}^3$ ). There were no recorded case of RN in patients with an increase in CTV at Fx3 relative to FxSim ( $n=3$ ). Figure 2a shows a case example of a patient with shrinkage in T1c CTV at Fx3 compared

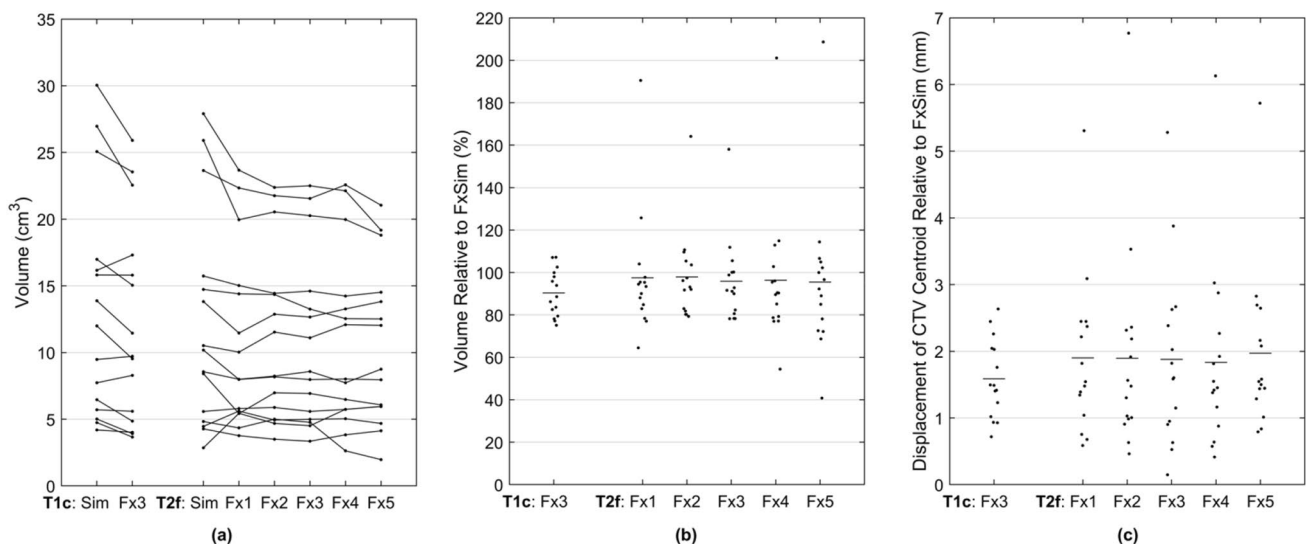
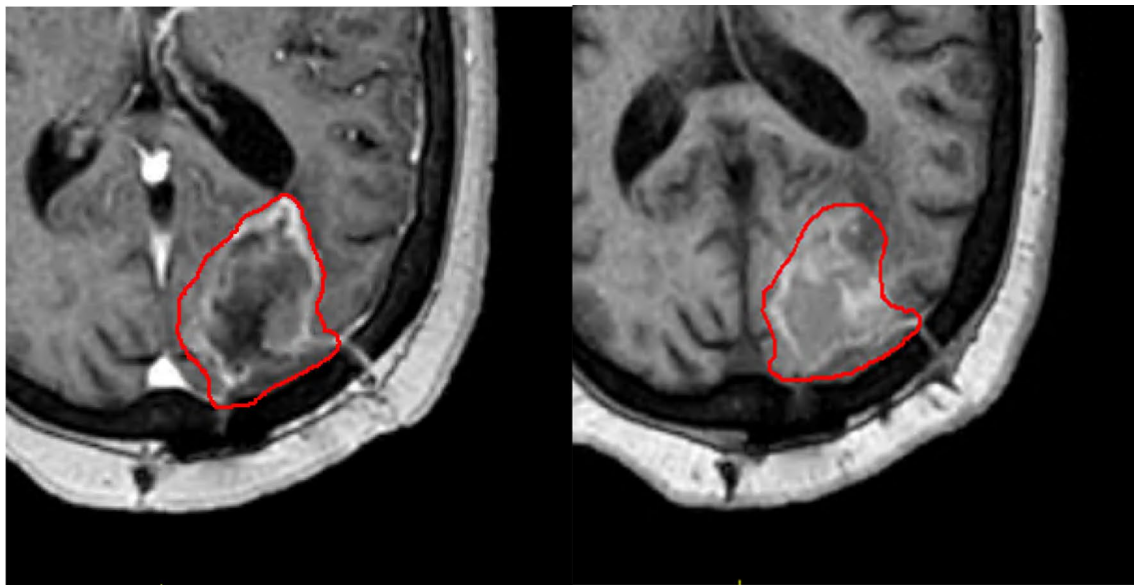
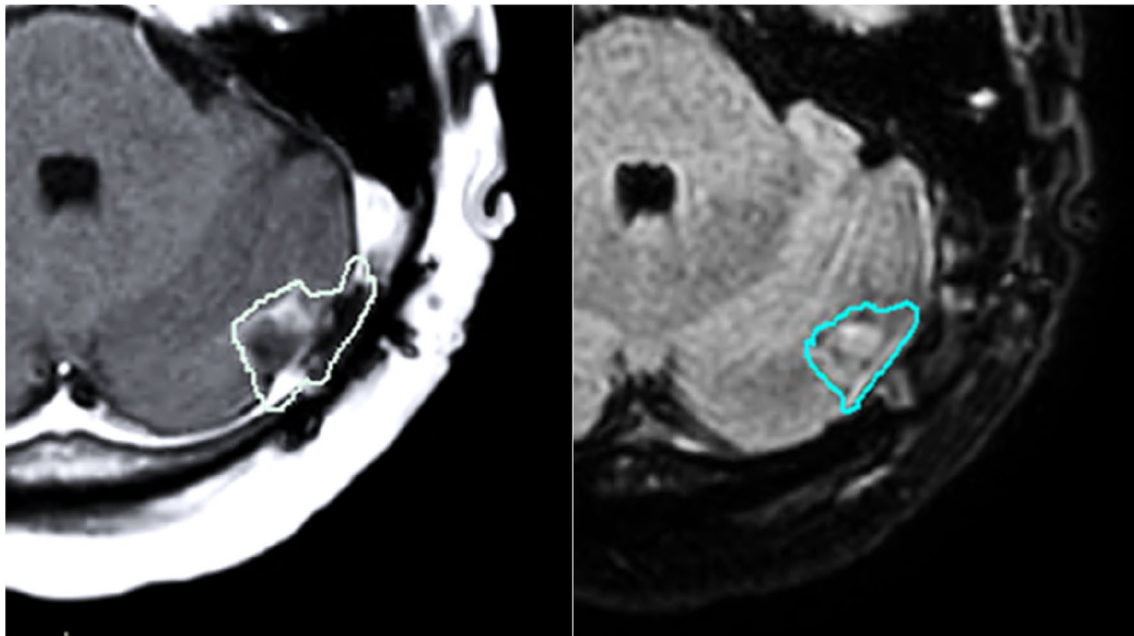


**Fig. 1** CTV volume on T1c at FxSim and Fx3, and T2f at FxSim and all five fractions **a** CTV volume relative to FxSim **b** and CTV centroid displacement from FxSim **c** shown for T1c Fx3 (column 1) and T2f Fx1 to Fx5 (columns 2–6). At each image/time point for

figure 1(b, c), measurements for  $n=15$  patients are shown randomly offset along the abscissa to improve visualization, with the horizontal line denotes the mean



(a)



(b)

**Fig. 2** Case examples of cavity dynamics and CTV contouring variability. **a** Case demonstrating cavity dynamics and change in CTV based on T1c at FxSim (left; volume,  $30.1\text{cm}^3$ ) and Fx3 (right; vol-

ume,  $25.9\text{cm}^3$ ). **b** Case demonstrating CTV contouring variability based on T1c (left; volume,  $6.5\text{cm}^3$ ) and T2f (right; volume,  $2.9\text{cm}^3$ ) at FxSim

to FxSim. Notably, one patient developed local progression at six months follow-up and recorded a CTV of  $7.7\text{cm}^3$  at FxSim and  $8.4\text{cm}^3$  at Fx3, with a relative change in CTV of +8.7% between the two time points.

### CTV contouring variability

To assess CTV contouring variability, we compared the CTV on T1c and T2f for each patient at FxSim using the following metrics.

### Absolute and relative volume

In 12/15 patients (80%), the T2f delineated CTV was smaller than the corresponding T1c delineated CTV. The median CTV on T1c was  $12.0\text{cm}^3$  (range, 1.2–30.1) and T2f was  $10.2\text{cm}^3$  (range, 2.9–27.9), reflecting a median % relative change in CTV of  $-6.0\%$  (range,  $-2$  to  $-55.8\%$ ). This volume reduction was statistically significant,  $p=0.040$ . The relationship between change in CTV contours from FxSim as quantified with T1c and T2f is shown in Fig. 3a. The largest volume reduction recorded were  $6.5\text{cm}^3$  on T1c and  $2.9\text{cm}^3$  on T2f, translating to a  $-55.8\%$  relative volume reduction as shown in Fig. 2b.

### Dice coefficient and Hausdorff distance

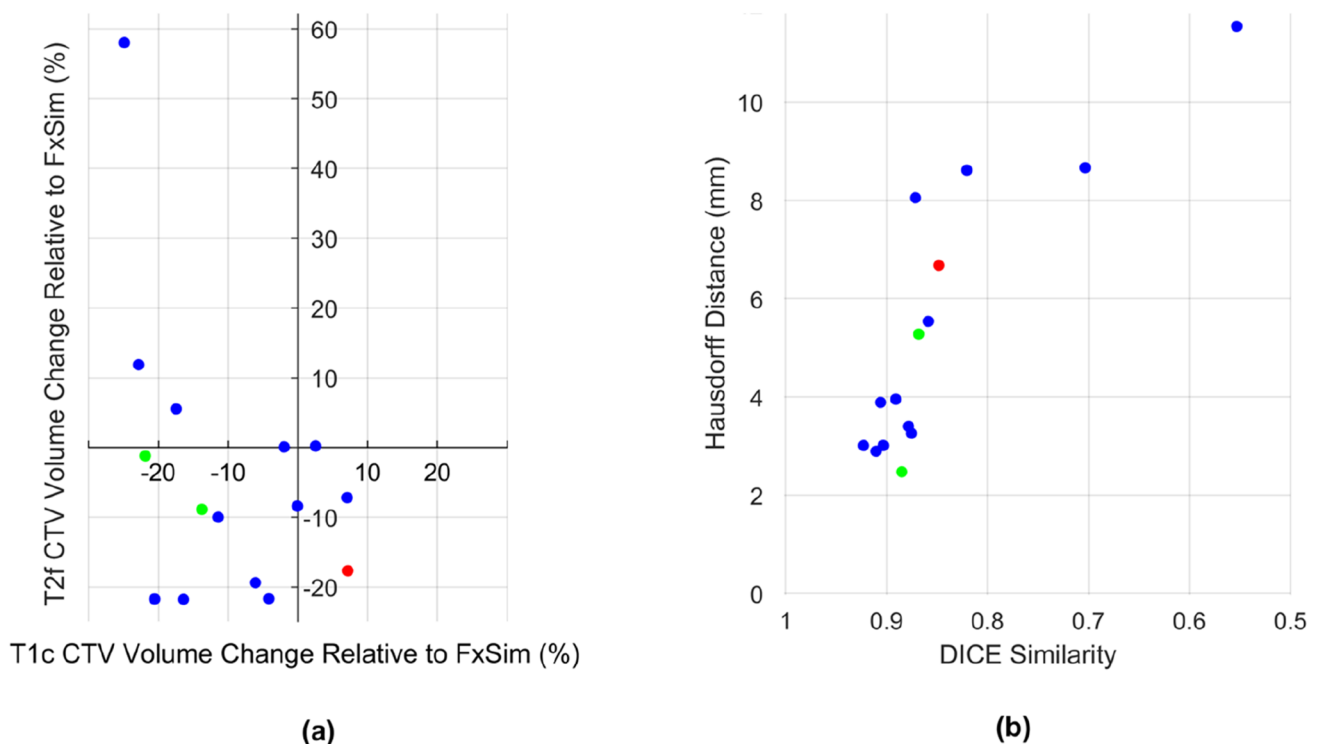
The mean DSC was  $0.85 \pm 0.10$ , and the mean HD was  $5.3 \pm 2.7$  mm when comparing CTVs contoured on T1c and T2f at FxSim. Table 2 illustrates the DSC and HD

values between CTV contoured on T1c and T2f at FxSim for all patients. The relationship between HD and DSC for CTV contouring variability is portrayed in Fig. 3b.

### Discussion

In the present study, we quantified the inter-fraction cavity dynamic changes on a 1.5 T MR LINAC (Elekta Unity, Elekta AB, Stockholm, Sweden) during HSRT to resected brain metastases and found statistically significant cavity dynamic changes, whereby the majority (80%) of our patients illustrated a reduction in T1c CTV volume at Fx3 relative to FxSim ( $p=0.009$ ). Additionally, CTV contouring variability was observed between T1c and T2f sequences, supporting that T1c should be used for accurate target delineation as per the consensus guidelines [9] during HSRT to resected brain metastases.

To our knowledge, no other published studies have evaluated the clinical utility of MR image guided radiation



- Denotes patients that developed radionecrosis
- Denotes the one patient that developed local progression

**Fig. 3** CTV contouring variability **a** Volume change relative to FxSim of the T1c (abscissa) and T2f (ordinal) contoured CTVs. **b** CTV contouring variability between T1c and T2f at FxSim. In this

panel, Hausdorff distance is plotted on the ordinal in ascending order, and DICE similarity along with the ordinal in descending order such that points closer to the lower-left indicate better contour agreement

**Table 2** Dice similarity coefficient and Hausdorff distance metrics for CTV (n = 15)

CTV Contouring variability	
T1c   T2f CTV at FxSim	
DSC	HD (mm)
0.87	8.1
0.85	6.6
0.91	2.9
0.82	8.4
0.88	3.4
0.88	2.5
0.86	5.4
0.70	8.7
0.92	3.0
0.90	3.0
0.88	3.3
0.89	3.9
0.55	11.4
0.91	3.9
0.87	5.3

DSC Dice similarity coefficient,  
HD Hausdorff distance

therapy (MRIgRT) systems to resected brain metastases. We postulate that individualized plan adaptation with online MRIgRT enables the possibility of identifying meaningful cavity dynamic changes, and treatment adaptation with adapt-to-shape (ATS) work flow on the MR LINAC would improve CTV coverage and limit unnecessary irradiation of normal brain tissue to mitigate the risk of RN. Dedicated MRIgRT systems enable such adaptation [14, 17–19], and in order to exploit the advantages of MRIgRT during HSRT for resected brain metastases, our present study aims to understand the cavity dynamics during HSRT and its clinical impact. This study also represents a prospective series looking at sequential MRI sequences at multiple time points and the utilization of specific metrics to evaluate cavity dynamics.

With regards to cavity dynamics, we observed a median % relative reduction of – 11.4% with CTV on T1c at Fx3 compared to FxSim ( $p=0.009$ ). Additionally, we observed a downward volume trend in terms of CTV contours on T2f from FxSim and over the course of HSRT. Dynamic change to the cavity has been demonstrated by prior literature. Alghamdi et al. observed a reduction in cavity volume by 28% for larger tumors (> 3 cm) at 22–42 days following surgery [20]. Similarly, Scharl et al. found that between postoperative MRI and planning MRI for HSRT (median 22 days), the cavity volume decreased, remained stable, and increased in 79.1%, 3.5%, and 17.4% of patients, respectively [21]. There are several other studies that support the hypothesis that cavities undergo dynamic volume changes following surgical resection [22, 23]. Collectively along with

our findings on cavity dynamics during HSRT, this indicates that strategies to adapt to changes in cavities during HSRT improve coverage of CTV and should be pursued in HSRT for resected brain metastases. Another strategy to overcome changes in cavity dynamics would be to utilise single fraction stereotactic radiosurgery (SRS) approach, as shown in these two larger prospective randomised trials [5, 6]. However, there are ongoing debate with respect to whether SRS or HSRT is superior for treating resected brain metastases. A recent analysis by Lehrer et al. found no significant differences in the 1-year local control between SRS vs HSRT (62.4% vs 85.7%,  $p=0.13$ ), although larger cavities are more likely to receive HSRT. The recruiting phase 3 randomised trial from the Alliance for Clinical Trials in Oncology (Clinicaltrials.gov: NCT04114981) [24], comparing the two regimens, which will provide its first result in 2025. It is noteworthy that the underlying mechanism driving cavity dynamics is multifactorial; resolution of the surgical cavity, collapse of brain tissue into surgical cavity, presence of oedema, accumulation of fluid or blood product and normal central nervous system motion could potentially contribute to the change [23, 25, 26]. The aforementioned factors driving cavity dynamics would need to be evaluated in future work as outcome data become evident.

The effect of CTV contraction also translates to an increase of normal brain irradiated and potentially risk of RN. In our study, there were 2 cases of RN on follow up and both cases had a reduction in CTV on T1c at Fx3 compared to FxSim. It is important to highlight that one of the patients with RN had previously received hippocampal avoidance WBRT, and it has been shown that prior WBRT is predictive of RN [27, 28]. A number of dose/volumetric parameters to normal brain have been demonstrated in the literature to predict the risk of RN [27], as outlined in the recent organ specific publication by the AAPM working group [29]. Factors correlated with a higher risk of RN include higher dose of radiotherapy, larger target volume and larger volume of normal brain receiving high dose irradiation [12, 27, 30, 31]. With respect to HSRT to resected brain metastases, volumetric constraints to brain which predict the risk of developing RN consist of V18Gy and V24Gy for 3 fractions regimen and V25Gy for 5 fractions regimen [12, 29]. We hypothesize that there may be a correlation between shrinkage in CTV, whereby a larger volume of normal brain is irradiated at Fx3 compared to FxSim and the risk of RN. In contrast, we have one recorded case of local progression on follow up MRI, and interestingly this patient had a relative increase in CTV of + 8.7% at Fx3 relative to FxSim. There was no tumour progression observed between FxSim and Fx3 and we speculate that under-coverage of CTV may have contributed to the case of local progression. These clinical scenarios, albeit in a small sample group, support the hypothesis that HSRT with

an ATS workflow on the MR LINAC may have potential benefits to the patient.

Finally, our study also investigated the feasibility of using T2f as a surrogate to define CTV by comparing the similarity of the CTV contour between T1c and T2f. T2f is a part of the standard set of sequences obtained on the MR LINAC. This sequence does lengthen the overall treatment time for our patients and no administration of contrast is required. Teyateeti et al. has concluded that T2 weighted MRI could provide an accurate resection cavity delineation without any detrimental clinical implications [13]. The authors also found that volume delineated with T2 weighted MRI is smaller than volume contoured on T1c sequences [13]. Comparably, our study found that 80% of our patients recorded a CTV reduction with a median % relative change of  $-6.0\%$  between T1c and T2f ( $p=0.040$ ). Furthermore, the mean DSC was  $0.85 \pm 0.10$ , and the mean HD was  $5.3 \pm 2.7$  mm when comparing CTV contoured on T1c and T2f at FxSim. Taken together, our study outlined that there is variability observed between CTV delineation on T2f and T1c at FxSim. The authors recommend the use of T1c for cavity delineation in line with the consensus guidelines [9]. Significant changes in T2f may be utilised as a prompt to obtaining T1c imaging but is not optimal alone for cavity delineation given the variability seen in our study. It is worth mentioning that not all cases in our study have documented a smaller CTV on T2f compared to T1c, which could potentially lead to under-coverage of CTV and impact on local control of tumor bed. We observed one particular case whereby the T1c CTV had a reduction of  $-24.9\%$  at FxSim relative to Fx3, but there was an increase in T2f CTV of  $64\text{--}108\%$  across all five fractions. In this specific case, the interface between the cavity and surrounding edema was difficult to differentiate as the T2 hyperintensity of the cavity appears very similar to the surrounding edema. Hence, the boundary was overestimated on the T2f contours. As a whole, we were unable to ascertain a consistent reason behind smaller volumes observed on the T2f compared to T1c, and this is a scope that would necessitate future prospective work.

One key limitation of our study is that we were only able to define CTVs on T1c at two time points (FxSim and Fx3) to minimize patients' exposure to cannulation and gadolinium contrast. The use of T2f CTVs at FxSim and all five fractions allows us to assess the overall trend of cavity dynamics, but our findings would only be validated by daily T1c images acquired on the MR LINAC. Further limitations include the difference in MRI imaging quality and gadolinium contrast uptake between FxSim and Fx3. Another limitation to consider is that the MR LINAC delivers non-coplanar intensity modulated radiotherapy (IMRT), which may have dosimetric impact on the plan in comparison to treatment with coplanar beams or volumetric modulated arc therapy (VMAT). Additionally, we cannot conclude a

relationship between specific treatment or tumor factors and cavity dynamics due to the small sample size and short-term follow-up. Nevertheless, online MRIgRT enables the possibility of identifying meaningful cavity dynamics changes and future study is underway to evaluate the clinical utility of the ATS workflow on improving CTV coverage and minimizing unnecessary irradiation of normal brain during HSRT to resected brain metastases.

## Conclusion

Statistically significant changes in cavity dynamics were observed during HSRT in resected brain metastases, supporting the use of MRIgRT and the rationale for the ATS workflow. We also observed CTV contouring variability between T1c and T2f sequences. Until outcomes are available to support the use of one sequence over another, we validate the use of the T1c sequence for CTV delineation and the use of T2f as an adjunct sequence to optimize target delineation.

**Author contributions** Concept: HT, HS, JS, Acquisition of data: All authors, Formal Analysis, Interpretation of data: HT, HS, JS, MR, Initial draft, revising draft, final draft: All authors, Project administration: AS, HS. All the authors are in agreement and accountable for all the aspects of the work.

**Funding** The authors did not receive financial support from any organization for the submitted work.

**Data Availability** Data will be made available on request to the corresponding author following the institutional ethics committee protocols.

## Declarations

**Conflict of interest** Mark Ruschin is a co-inventor/owns intellectual property specific to the image-guidance system on the Gamma Knife Icon outside the submitted work. Hany Soliman has received travel accommodations/expenses and honoraria from Elekta AB outside the submitted work. Arjun Sahgal is an advisor/consultant for AbbVie, Merck, Roche, Varian, Elekta AB, BrainLAB, and VieCure; is a board member of the International Stereotactic Radiosurgery Society; is co-chair of the AO Spine Knowledge Forum Tumor; has conducted educational seminars for Elekta AB, Accuray Inc, Varian, BrainLAB, and Medtronic Kyphon; has received research grants from Elekta AB and travel accommodations/expenses from Elekta AB, Varian, and BrainLAB; and is a member of the Elekta MR-Linac Research Consortium, Elekta Spine, Oligometastases, and Linac-based SRS Consortia. Chia-Lin Tseng has received travel accommodations/expenses and honoraria from Elekta AB and belongs to the Elekta MR-Linac Research Consortium. The remaining authors reported no disclosures or conflicts of interest related to submitted work.



## References

- Patchell RA, Tibbs PA, Walsh JW, Dempsey RJ, Maruyama Y, Kryscio RJ et al (1990) A randomized trial of surgery in the treatment of single metastases to the brain. *N Engl J Med* 322(8):494–500
- Kocher M, Soffietti R, Abacioglu U, Villa S, Fauchon F, Baumert BG et al (2011) Adjuvant whole-brain radiotherapy versus observation after radiosurgery or surgical resection of one to three cerebral metastases: results of the EORTC 22952–26001 study. *J Clin Oncol* 29(2):134–141
- Chang EL, Wefel JS, Hess KR, Allen PK, Lang FF, Kornguth DG et al (2009) Neurocognition in patients with brain metastases treated with radiosurgery or radiosurgery plus whole-brain irradiation: a randomised controlled trial. *Lancet Oncol* 10(11):1037–1044
- Brown PD, Jaeckle K, Ballman KV, Farace E, Cerhan JH, Anderson SK et al (2016) Effect of radiosurgery alone vs radiosurgery with whole brain radiation therapy on cognitive function in patients with 1 to 3 brain metastases: a randomized clinical trial. *JAMA* 316(4):401–409
- Mahajan A, Ahmed S, McAleer MF, Weinberg JS, Li J, Brown P et al (2017) Post-operative stereotactic radiosurgery versus observation for completely resected brain metastases: a single-centre, randomised, controlled, phase 3 trial. *Lancet Oncol* 18(8):1040–1048
- Brown PD, Ballman KV, Cerhan JH, Anderson SK, Carrero XW, Whitton AC et al (2017) Postoperative stereotactic radiosurgery compared with whole brain radiotherapy for resected metastatic brain disease (NCCTG N107C/CEC.3): a multicentre, randomised, controlled, phase 3 trial. *Lancet Oncol* 18(8):1049–1060
- Soliman H, Myrehaug S, Tseng CL, Ruschin M, Hashmi A, Mainprize T et al (2019) Image-guided, linac-based, surgical cavity-hypofractionated stereotactic radiotherapy in 5 daily fractions for brain metastases. *Neurosurgery* 85(5):E860–E869
- Eitz KA, Lo SS, Soliman H, Sahgal A, Theriault A, Pinkham MB et al (2020) Multi-institutional analysis of prognostic factors and outcomes after hypofractionated stereotactic radiotherapy to the resection cavity in patients with brain metastases. *JAMA Oncol* 6(12):1901
- Soliman H, Ruschin M, Angelov L, Brown PD, Chiang VLS, Kirkpatrick JP et al (2018) Consensus contouring guidelines for postoperative completely resected cavity stereotactic radiosurgery for brain metastases. *Int J Radiat Oncol Biol Phys* 100(2):436–442
- Eaton BR, LaRiviere MJ, Kim S, Prabhu RS, Patel K, Kandula S et al (2015) Hypofractionated radiosurgery has a better safety profile than single fraction radiosurgery for large resected brain metastases. *J Neurooncol* 123(1):103–111
- Specht HM, Kessel KA, Oechsner M, Meyer B, Zimmer C, Combs SE (2016) HFSRT of the resection cavity in patients with brain metastases. *Strahlenther Onkol* 192(6):368–376
- Minniti G, Esposito V, Clarke E, Scaringi C, Lanzetta G, Salvati M et al (2013) Multidose stereotactic radiosurgery (9 Gy x 3) of the postoperative resection cavity for treatment of large brain metastases. *Int J Radiat Oncol Biol Phys* 86(4):623–629
- Teyateeti A, Brown PD, Mahajan A, Laack NN, Pollock BE (2020) Brain metastases resection cavity radio-surgery based on T2-weighted MRI: technique assessment. *J Neurooncol* 148(1):89–95
- Hall WA, Paulson ES, van der Heide UA, Fuller CD, Raaymakers BW, Legendijk JJW et al (2019) The transformation of radiation oncology using real-time magnetic resonance guidance: A review. *Eur J Cancer* 122:42–52
- de Mol SR, van Otterloo CJP, Blezer ELA, Akhlat H, Brown K, Choudhury A et al (2021) Patterns of Care, tolerability, and safety of the first cohort of patients treated on a novel high-field mr-linac within the momentum study: initial results from a prospective multi-institutional registry. *Int J Radiat Oncol Biol Phys* 111:867–875
- Sneed PK, Mendez J, Vemer-van den Hoek JG, Seymour ZA, Ma L, Molinaro AM et al (2015) Adverse radiation effect after stereotactic radiosurgery for brain metastases: incidence, time course, and risk factors. *J Neurosurg* 123(2):373–386
- Cao Y, Tseng CL, Balter JM, Teng F, Parmar HA, Sahgal A (2017) MR-guided radiation therapy: transformative technology and its role in the central nervous system. *Neuro Oncol* 19(2):ii16–ii29
- Mutic S, Dempsey JF (2014) The ViewRay system: magnetic resonance-guided and controlled radiotherapy. *Semin Radiat Oncol* 24(3):196–199
- Fallone BG (2014) The rotating biplanar linac-magnetic resonance imaging system. *Semin Radiat Oncol* 24(3):200–202
- Alghamdi M, Hasan Y, Ruschin M, Atenafu EG, Myrehaug S, Tseng CL et al (2018) Stereotactic radiosurgery for resected brain metastasis: Cavity dynamics and factors affecting its evolution. *J Radiosurg SBRT* 5(3):191–200
- Scharl S, Kirstein A, Kessel KA, Duma MN, Oechsner M, Straube C et al (2019) Cavity volume changes after surgery of a brain metastasis-consequences for stereotactic radiation therapy. *Strahlenther Onkol* 195(3):207–217
- Atalar B, Choi CY, Harsh GRT, Chang SD, Gibbs IC, Adler JR et al (2013) Cavity volume dynamics after resection of brain metastases and timing of postresection cavity stereotactic radiosurgery. *Neurosurgery* 72(2):180–185
- Jarvis LA, Simmons NE, Bellerive M, Erkmen K, Eskey CJ, Gladstone DJ et al (2012) Tumor bed dynamics after surgical resection of brain metastases: implications for postoperative radiosurgery. *Int J Radiat Oncol Biol Phys* 84(4):943–948
- ClinicalTrials.gov. Single Fraction Stereotactic Radiosurgery Compared With Fractionated Stereotactic Radiosurgery in Treating Patients With Resected Metastatic Brain Disease. NCT04114981. Assessed Nov 2021 [
- Wernicke AG, Hirschfeld CB, Smith AW, Taube S, Yondorf MZ, Parashar B et al (2017) Clinical outcomes of large brain metastases treated with neurosurgical resection and intraoperative cesium-131 brachytherapy: results of a prospective trial. *Int J Radiat Oncol Biol Phys* 98(5):1059–1068
- Ahmed S, Hamilton J, Colen R, Schellinghout D, Vu T, Rao G et al (2014) Change in postsurgical cavity size within the first 30 days correlates with extent of surrounding edema: consequences for postoperative radiosurgery. *J Comput Assist Tomogr* 38(3):457–460
- Faruqi S, Ruschin M, Soliman H, Myrehaug S, Zeng KL, Husain Z et al (2020) Adverse radiation effect after hypofractionated stereotactic radiosurgery in 5 daily fractions for surgical cavities and intact brain metastases. *Int J Radiat Oncol Biol Phys* 106(4):772–779
- Kohutek ZA, Yamada Y, Chan TA, Brennan CW, Tabar V, Gutin PH et al (2015) Long-term risk of radionecrosis and imaging changes after stereotactic radiosurgery for brain metastases. *J Neurooncol* 125(1):149–156
- Milano MT, Grimm J, Niemierko A, Soltys SG, Moiseenko V, Redmond KJ et al (2021) Single- and multifraction stereotactic radiosurgery dose/volume tolerances of the brain. *Int J Radiat Oncol Biol Phys* 110(1):68–86
- Jhaveri J, Chowdhary M, Zhang X, Press RH, Switchenko JM, Ferris MJ et al (2018) Does size matter? Investigating the optimal planning target volume margin for postoperative stereotactic radiosurgery to resected brain metastases. *J Neurosurg* 130(3):797–803
- Blonigen BJ, Steinmetz RD, Levin L, Lamba MA, Warnick RE, Breneman JC (2010) Irradiated volume as a predictor of brain radionecrosis after linear accelerator stereotactic radiosurgery. *Int J Radiat Oncol Biol Phys* 77(4):996–1001

**Publisher's Note** Springer Nature remains neutral with regard to jurisdictional claims in published maps and institutional affiliations.